AN INVESTIGATION CONCERNING OPTIMAL
DESIGN OF SOLID ELASTIC PLATES

KENG-TUNG CHENG† and NIELS OLHOFF

Department of Solid Mechanics, The Technical University of Denmark, Lyngby, Denmark

Abstract—We consider the problem of maximizing the integral stiffness of solid elastic plates described by thin plate theory. Assuming the material volume and plate domain to be given, we use the plate thickness function as the design variable and take both maximum and minimum allowable thickness values into account. On the basis of a convenient tensorial formulation of the problem, where the governing equations are derived by variational analysis and constitute necessary conditions for stationarity, we develop an efficient and quite general numerical algorithm by means of which a number of stationary solutions for rectangular and axisymmetric annular plates with various boundary conditions are obtained.

These numerical results enable us to investigate the optimization problem itself in terms of its major parameters, particularly the maximum and minimum values specified for the plate thickness. For problems associated with large ratios between these constraint values, plate designs with significant integral stiffeners are obtained. We find however, that these designs are only local optima and that a global optimal plate thickness function does generally neither exist within the class of smooth functions nor within the class of smooth functions with a finite number of discontinuities. In order to determine a global optimal solution associated with given thickness constraint values, it is therefore necessary to change the optimal design formulation. With implications for a number of similar two-dimensional optimization problems, our results offer valuable indications of the lines along which such changes should be performed.

INTRODUCTION

Optimal design problems for thin, solid elastic plates of non-uniform thickness are considerably complicated by an inherent cubic relationship between the plate bending rigidity and thickness. This non-linear relationship is the cause of the difficulty[1-3] that the field equations for stationarity are only necessary conditions for optimality and do not ensure global optimality of a possible solution. Moreover, due to the cubic relationship mentioned, the governing field equations for the plate become a highly nonlinear and strongly coupled system of integro-partial differential equations, the complexity of which readily excludes the possibility of closed form solutions. The search for solutions and investigations of many significant features of plate optimization problems as well, must therefore be based on numerical methods specially developed for these purposes.

Numerical solutions to geometrically unconstrained solid plate optimization problems, i.e. problems where no constraints are specified for the plate thickness function, are published in [4-8]. These solutions all have smoothly varying thickness distributions, but as is argued in different ways in [2,3,7,9-11], plate designs with integral stiffeners will be associated with more optimal properties. The advantage of a direct use of stiffeners for reinforcement has been demonstrated in different contexts in [12-16]. Smooth, stationary solutions obtained to geometrically unconstrained formulations for optimal design must consequently be considered as local optimal solutions, see [2,3,7,9,17,18].

Thus, we are confronted with the paradoxical situation that optimal plate designs must be expected to have integral stiffeners, but that such solutions have yet not been obtained by optimization. This paradox is previously studied in [17] by way of introducing suitable singularities into a geometrically unconstrained plate optimization problem. This problem was thus shown to possess several local optimal solutions with stiffener-like thickness distributions between the singularities. It was also found in [17] that the optimal characteristics of the local optimal solutions increase rapidly with the number of stiffeners contained in the solutions, but that a global optimal solution does not exist when no constraints are prescribed for the plate thickness function. The latter result is later confirmed mathematically in [2,3].

It is the objective of the present paper to investigate a reformulation of the plate optimization problem, where both maximum and minimum constraints are considered for the

†Visiting from the Dept. of Solid Mechanics, The Dalian Engineering Institute, Dalian, The People's Republic of China.

plate thickness function. As before, the available volume, material, domain and boundary conditions for the plate are assumed to be given. We consider the problem of maximizing the stiffness (minimizing the compliance) subject to a given transverse load distribution on the plate. To some extent, this problem is less complicated than designing with respect to other objectives, but it contains all the significant features that are inherent in optimal design of plates. Maximum stiffness design of solid plates has previously been considered in [3, 4, 8, 11, 16, 19–21], of sandwich plates in [22, 23] and of other structures in, e.g. [24–26].

In Section 1, we state the plate equations and three sets of homogeneous boundary conditions in tensor form. This is the outset for the derivation in Section 2 of a general set of necessary conditions for optimality from the principle of minimum potential energy by variational analysis. In Section 3, we then develop a stable and effective numerical solution procedure based on successive iterations, which can be used for any particular coordinate system chosen for the plate. In Section 4 the set of tensorial governing equations are specialized to Cartesian coordinates and solved for simply supported and clamped rectangular plates by means of the aforementioned numerical procedure. Using polar coordinates as a reference frame in Section 5, we present a number of results for axisymmetric annular plates with various combinations of boundary conditions. Here, the loading is assumed to vary harmonically in the circumferential direction, which implies that the governing equations for optimality are reduced to a set of ordinary integro-differential equations.

The numerical results presented in Sections 4 and 5 display significant features: a definitive tendency towards formation of stiffeners and the existence of different local optimal plate designs. Furthermore, for problems associated with large ratios between the maximum and minimum thickness constraints, a global optimal design does not seem to exist within the class of thickness functions considered in the present formulation; our results indicate, as is discussed in Section 6, that such a design should be sought within a class of plates that has an infinite number of infinitely thin stiffeners.

1. PLATE EQUATIONS IN TENSOR FORM

We consider a thin, solid, elastic plate of variable thickness, whose mid-plane occupies a given domain Ω with the contour ω in the $x^1 - x^2$-plane of some three-dimensional coordinate system x^i, the x^3-axis of which is assumed to be perpendicular to the $x^1 - x^2$-plane. The plate is assumed to be loaded transversely by a given static load of intensity $p(x^1, x^2)$, and the equation of equilibrium in the x^3-direction can then be written in the general form [27, 28]

$$d_\alpha d_\beta M^{\alpha\beta} = p. \tag{1}$$

Here and in the following, Greek indices take values 1 and 2 and repeated indices imply summation.

In eqn (1), d_α denotes the operator of covariant differentiation with respect to the coordinate of index α, and $M^{\alpha\beta}$ is the contravariant, second order moment tensor

$$M^{\alpha\beta} = D\{(1 - \nu)d^\alpha d^\beta w + \nu a^{\alpha\beta} d_\gamma d^\gamma w\}, \tag{2}$$

where the scalar function $w(x^\alpha)$ denotes the plate deflection in the x^3-direction, $a^{\alpha\beta}$ is the contravariant metric tensor for the plate mid-plane coordinates x^α and $d^\alpha = a^{\alpha\gamma} d_\gamma$ is the operator of contravariant differentiation.

The function $D(x^\alpha)$ in eqn (2) identifies the plate bending rigidity

$$D = \frac{Eh^3}{12(1 - \nu^2)}. \tag{3}$$

Within thin plate theory, this is a scalar function (i.e. independent of orientation) and it is noted to be cubic in the thickness function $h(x^\alpha)$ for solid plates. The constants E and ν denote Young's modulus and Poisson's ratio, respectively, of the plate material.

By substituting eqn (2) into eqn (1), we obtain the following fourth order, partial differential equation for the deflection function $w(x^\alpha)$ of a plate of variable thickness

$$d_\alpha d_\beta [D\{(1-\nu)d^\alpha d^\beta w + \nu a^{\alpha\beta} d_\gamma d^\gamma w\}] = p. \tag{4}$$

At the contour ω of the plate, we consider the possibility that either of the following three sets of linear, homogeneous boundary conditions may be prescribed, namely, the conditions for a simple supported plate edge

$$w = 0, \quad M_B(w) = 0 \quad x^\alpha \in \omega, \tag{5a}$$

the conditions for a clamped edge

$$w = 0, \quad \psi(w) = 0 \quad x^\alpha \in \omega, \tag{5b}$$

or the conditions for a free edge (assuming the plate to be supported elsewhere)

$$M_B(w) = 0, \quad Q(w) = 0 \quad x^\alpha \in \omega. \tag{5c}$$

In (5b), $\psi = n^\alpha d_\alpha w$ identifies the scalar slope of the deflection w normal to the curve ω, and in (5a) and (5c),

$$M_B = M^{\alpha\beta} n_\alpha n_\beta \tag{6}$$

and

$$Q = -n_\alpha d_\beta M^{\alpha\beta} - \frac{\partial(M^{\alpha\beta} t_\alpha n_\beta)}{\partial\omega} \tag{7}$$

represent, respectively, the effective bending moment and the effective (Kirchhoff) shear force per unit length of the curve ω. Here, n_α and t_α denote, respectively, the outward unit normal vector and the unit tangential vector in the x^α plane to the curve ω.

By means of the expressions for ψ, M_B and Q given above, and the expression for $M^{\alpha\beta}$ in eqn (2), all the boundary conditions (5a)–(5c) can readily be written in terms of w.

2. GENERAL FORMULATION OF THE OPTIMIZATION PROBLEM

Using the plate thickness function $h(x^\alpha)$ as the design variable, it is now our objective to maximize the integral stiffness of the plate subject to a given transverse load distribution $p(x^\alpha)$ and given boundary conditions. This problem is equivalent to minimization of the compliance

$$\pi = \int_\Omega pw \, d\Omega, \tag{8}$$

that is, the work done by the applied forces.

The optimization is to be performed under the condition that the total volume of plate material

$$V = \int_\Omega h \, d\Omega \tag{9}$$

is prescribed. The domain Ω and the material constants E and ν of the elastic plate are assumed to be given as well.

In addition to the integral constraint (9) for our design variable $h(x^\alpha)$, we also assume that a maximum and a minimum allowable value (h_{max} and h_{min}, respectively), are specified for h, i.e.

$h_{max} \leq h(x^\alpha) \leq h_{min}$. These inequality constraints are easily transformed into equality constraints

$$h_{max} - h = \sigma^2 \tag{10}$$

$$h - h_{min} = \tau^2 \tag{11}$$

by means of the real slack variables $\sigma(x^\alpha)$ and $\tau(x^\alpha)$.

We now apply a variational formulation of the optimization problem stated above and construct an augmented functional π^*,

$$\pi^* = \int_\Omega pw \, d\Omega - \int_\Omega \eta[d_\alpha d_\beta[D\{(1-\nu)d^\alpha d^\beta w + \nu a^{\alpha\beta} d_\gamma d^\gamma w\}] - p] \, d\Omega + \Lambda \left[\int_\Omega h \, d\Omega - V\right]$$

$$- \int_\Omega \lambda[h - h_{max} + \sigma^2] \, d\Omega - \int_\Omega \kappa[h_{min} - h + \tau^2] \, d\Omega \tag{12}$$

where the plate differential eqn (4), the volume constraint (9), the geometric maximum constraint (10) and minimum constraint (11), respectively, are adjoined to the functional π of eqn (8) by means of Lagrangian multipliers $\eta(x^\alpha)$, Λ, $\lambda(x^\alpha)$ and $\kappa(x^\alpha)$. The principle of stationary potential energy and the introduction of the Lagrangian multipliers permit us to take independent variations of π^* with respect to its variables in the following.

The set of necessary governing equations for our optimization problem now consists of the Euler–Lagrange equations expressing stationarity of π^* for arbitrary admissible variation δw, δh, $\delta \sigma$ and $\delta \tau$, in addition to the constraint eqns (4), (9), (10), (11), and the particular set of boundary conditions (5a), (5b) or (5c) under consideration.

As is shown in the Appendix, the condition of stationarity of π^* with respect to variation of w leads to the result that the Lagrangian multiplier function $\eta(x^\alpha)$ satisfies the same differential eqn (4) and particular set of boundary conditions (5a), (5b) or (5c) as does the function $w(x^\alpha)$. Hence, we have

$$\eta(x^\alpha) \equiv w(x^\alpha). \tag{13}$$

When deriving the condition of stationarity† of π^* with respect to variation of the design variable $h(x^\alpha)$, the so-called *optimality condition*, it is useful to write the second integral on the r.h.s. of eqn (12) in terms of $M^{\alpha\beta}$ by means of eqn (2), and to eliminate η by means of (13). Performing the variation with subsequent application of the divergence theorem and the boundary conditions for $w(x^\alpha)$ as shown in the Appendix, we arrive at the result

$$\frac{\partial D}{\partial h} \frac{1}{(1-\nu^2)D^2} [(1+\nu)M^{\alpha\beta}M_{\alpha\beta} - \nu M_\alpha^\alpha M_\beta^\beta] = \Lambda - \lambda + \kappa, \tag{14}$$

where $M^{\alpha\beta}$ is the moment tensor corresponding to the deflection function $w(x^\alpha)$. If we introduce the design variable $h(x^\alpha)$ by means of eqn (3) and redefine Lagrangian multipliers Λ, $\lambda(x^\alpha)$ and $\kappa(x^\alpha)$ by a simple scaling factor, the optimality condition (14) can be written in the form

$$h^{-4}[(1+\nu)M^{\alpha\beta}M_{\alpha\beta} - \nu M_\alpha^\alpha M_\beta^\beta] = \Lambda - \lambda + \kappa. \tag{15}$$

The variation of π^* with respect to σ and τ, respectively, gives the switching equations

$$\lambda \sigma = 0 \tag{16}$$

and

$$\kappa \tau = 0. \tag{17}$$

†The condition is necessary but not sufficient for global optimality.

Comparing these equations with the defining eqns (10) and (11) for the slack variables $\sigma(x^\alpha)$ and $\tau(x^\alpha)$, we are able to deduce the following results by studying possible combinations of σ and τ: If $\sigma \neq 0$ and $\tau \neq 0$, then we have $\lambda = \kappa = 0$ and $h_{max} < h < h_{min}$, i.e. the thickness function is unconstrained at the point considered. If $\sigma \neq 0$ and $\tau = 0$, then $\kappa = 0$ and $h = h_{min}$, that is, the thickness is constrained from below. If we have $\sigma = 0$ and $\tau \neq 0$, then $\lambda = 0$ and $h = h_{max}$, i.e. h is constrained from above. The combination $\sigma = \tau = 0$ is not possible since we assume $h_{max} > h_{min}$.

The above results enable us to eliminate the functions λ, κ, σ, τ and instead introduce the unions Ω_{ca}, Ω_u and Ω_{cb} of subdomains in Ω ($\Omega = \Omega_{ca} \cup \Omega_u \cup \Omega_{cb}$), where the plate thickness $h(x^\alpha)$ is constrained from *above*, *unconstrained* and *constrained* from *below*, respectively. Introducing the short-hand notation g for the scalar function

$$g(x^\alpha) = (1 + \nu)M^{\alpha\beta}M_{\alpha\beta} - \nu M_\alpha{}^\alpha M_\beta{}^\beta, \qquad (18)$$

we can then write the following convenient formula for the plate thickness function h,

$$h(x^\alpha) = \begin{cases} h_{max} & \text{if} \quad (g(x^\alpha)/\Lambda)^{1/4} \geq h_{max}, \quad x^\alpha \in \Omega_{ca} \\ (g(x^\alpha)/\Lambda)^{1/4}, & x^\alpha \in \Omega_u \\ h_{min} & \text{if} \quad (g(x^\alpha)/\Lambda)^{1/4} \leq h_{min}, \quad x^\alpha \in \Omega_{cb} \end{cases} \qquad (19)$$

where the expression for h in the (unions of) unconstrained subdomain(s) Ω_u (with $\lambda = \kappa = 0$) follows from eqns (15) and (18).

Now we only need a suitable expression for the Lagrangian multiplier Λ. Substituting eqn (19) into the volume constraint (9) and solving for Λ, we obtain

$$\Lambda = \left[\frac{\displaystyle\int_{\Omega_u} g(x^\alpha)^{1/4}\, d\Omega}{V - h_{min} \displaystyle\int_{\Omega_{cb}} d\Omega - h_{max} \displaystyle\int_{\Omega_{ca}} d\Omega} \right]^4. \qquad (20)$$

In summary, the complete system of necessary conditions for our optimization problem consists of eqns (2)–(4), (8) and (18)–(20), together with a particular set of the boundary conditions (5a), (5b) or (5c). This system of equations is seen to constitute a coupled, non-linear integro-partial differential boundary value problem with unknown interior boundaries, and closed form solutions cannot be expected. The principal unknowns to be determined are the minimum compliance π, the associated deflection $w(x^\alpha)$ and the thickness function $h(x^\alpha)$, of the optimal plate, which in turn require determination of the Lagrangian multiplier Λ and the subdomains Ω_{ca}, Ω_u and Ω_{cb}.

The given quantities for a particular problem can be summarized as the following: the type of coordinate system x^i, the plate domain Ω with contour ω and transverse static load distribution $p(x^\alpha)$, the total plate volume V, the minimum and maximum allowable values h_{min} and h_{max} for the plate thickness, and the constants E and ν for the plate material.

3. SOLUTION PROCEDURE BASED ON SUCCESSIVE ITERATIONS

In order to solve the governing non-linear, integro-partial differential boundary value problem, i.e. eqns (2)–(4), (8) and (18)–(20), which, together with a given set of boundary conditions (5a), (5b) or (5c), constitute the mathematical formulation of our plate optimization problem, we apply a numerical solution procedure based on successive iterations.

The general iteration scheme constructed and used as a basis for obtaining all the numerical results presented in this paper has the following form:

START   Take $h(x^\alpha)$ arbitrarily together with Ω_{ca}, Ω_u and Ω_{cb} such that $\int_{\Omega_u} d\Omega > 0$.

  I   Compute $D(x^\alpha)$ by eqn (3).

  II Solve $w(x^\alpha)$ from discretized version of differential eqn (4) and boundary conditions (5a), (5b) or (5c).

III Compute $M^{\alpha\beta}$ by eqn (2), determine $M_{\alpha\beta}$ and $M_\alpha{}^\alpha$, and compute $g(x^\alpha)$ by eqn (18).

IV Compute Λ by eqn (20).

V Determine $h(x^\alpha)$ together with Ω_{ca}, Ω_u and Ω_{cb} from eqn (19).

VI Go to IV if $h(x^\alpha)$ has not converged in the inner iteration loop IV–VI.

VII Go to I if $h(x^\alpha)$ and hence all other iterates have not converged in the main iteration loop I–VII.

VIII Compute π by eqn (8).

END

In this scheme, the functions are iterates represented by their discrete values at a number of fixed mesh points in the domain Ω and at its contour ω embedded in the x^α plane of a given coordinate system. For a given set of mesh points, the sequence of iterates is found to converge rapidly towards the numerical solution, especially if the ratio h_{max}/h_{min} is not taken too large (i.e. greater than about 5). However, as will be outlined and discussed in the subsequent sections, our numerical study reveals that in some problems, i.e. for given Ω, $p(x^\alpha)$, V, h_{min}, h_{max}, E and v, the numerical solution to the discretized problem is significantly dependent on the fineness of the grid used in the computations.

4. RECTANGULAR PLATES

When dealing with rectangular plates, it is convenient to select x^i as a Cartesian coordinate system. Then the components of the metric tensor for the plate mid-surface are given by

$$a^{\alpha\beta} = a_\beta{}^\alpha = a_{\alpha\beta} = \begin{Bmatrix} 1 & 0 \\ 0 & 1 \end{Bmatrix}, \tag{21}$$

which implies that no distinction is necessary between contravariant, mixed and covariant components of similar indices of any Cartesian tensor and that the Christoffel symbols vanish, such that contravariant and covariant differentiation both reduce to usual partial differentiation.

Denoting the x^1, x^2 and x^3 axes of the Cartesian coordinate system by x, y and z, respectively, the compact differential equation (4) for plates of variable thickness can be written in the familiar expanded form[29]

$$(Dw_{,xx})_{,xx} + (Dw_{,yy})_{,yy} + v(Dw_{,xx})_{,yy} + v(Dw_{,yy})_{,xx} + 2(1-v)(Dw_{,xy})_{,xy} = p, \tag{22}$$

where commas denote partial differentiation with respect to succeeding coordinate(s). Equation (2) can be expressed in the traditional form

$$M_{xx} = D(w_{,xx} + vw_{,yy}), \quad M_{yy} = D(w_{,yy} + vw_{,xx}), \quad M_{xy} = D(1-v)w_{,xy}, \tag{23}$$

where $M_{xx}(= M^{11} = M_1{}^1 = M_{11})$ and $M_{yy}(= M^{22} = M_2{}^2 = M_{22})$ are the physical bending moments and $M_{xy}(= M^{12} = M^{21} = M_1{}^2$, etc.) the physical twisting moment (all per unit length) in the plate.

The characteristic quadratic expression termed g in eqn (18) can be written out as

$$g(x^\alpha) = (M_{xx} + M_{yy})^2 + 2(1+v)[M_{xy}^2 - M_{xx}M_{yy}], \tag{24}$$

and substituting eqn (24) with M_{xx}, M_{yy} and M_{xy} given by (23) into eqn (15), the optimality condition reduces to the familiar form[20]

$$h^2[(\Delta w)^2 + 2(1-v)[w_{,xy}^2 - w_{,xx}w_{,yy}]] = \Lambda, \tag{25}$$

in the unconstrained subdomain Ω_u. In eqn (25), Δ denotes the Laplacian operator $\Delta(\;) = (\;)_{,xx} + (\;)_{,yy}$, and the original Lagrangian multiplier Λ has been scaled.

Performing the numerical solution procedure for rectangular plates, we choose the x and y axes of the Cartesian coordinate system along two intersecting plate edges and introduce a rectangular grid in the plate domain with equidistant spacing in the x and y directions.

To solve the Cartesian version (22) of the plate eqn (4) together with a given set of boundary conditions in Step II of the iteration scheme outlined in Section 2, a finite difference method is used. Since stiffener-like thickness variation is to be expected as a result of our optimization, the finite difference scheme is developed on the basis of low order polynomial approximations and care has been taken to avoid as much as possible the use of approximations that implicitly assume continuity and differentiability across the interior boundaries between constrained and unconstrained subdomains, where first order derivatives of the thickness function and higher order derivatives of the deflection are discontinuous.

Results and discussion

We now present some thickness distributions obtained for square, solid, elastic plates that are acted on by uniformly distributed static loading and optimized for maximum stiffness (minimum compliance).

Figure 1 illustrates a square plate whose edges are all simply supported, and the result shown in Fig. 2 is for a plate with all edges clamped. The constrained and uncontrained subdomains for the plate thickness functions are easily identified in the figures. Both results are obtained for a comparatively small ratio, $h_{max}/h_{min} = 1.5$, between the maximum and minimum thickness constraints, and the volume assigned to the plates is given by $h_u/h_{min} = 1.25$, where h_u designates the thickness corresponding to uniform distribution of the plate volume. Poisson's ratio for the plate material is taken to be $\nu = 0.25$. The compliance π of the simply supported plate in Fig. 1 is 82.4% of the compliance π_u of a uniform, simply supported plate with the same volume, side lengths, material and loading and the compliance of the clamped plate in Fig. 2 is 70.7% of the compliance of a corresponding uniform, clamped plate. A grid consisting of 10 × 10 equally spaced points for a quarter plate is used in the numerical solution procedure.

The build-up of material in the corner of the simply supported plate in Fig. 1 is noticeable since it can be shown analytically that the thickness function vanishes along simply supported edges and particularly at the corner between such edges, if no minimum constraint is specified for the plate thickness (see Ref. [7, 19] for a slightly different problem). However, the physical conditions at the simply supported plate corner crucially depend on whether or not a minimum thickness constraint is considered in the formulation for optimal design; in the case where no minimum constraint is specified, it can be shown by means of an analytical expansion of the solution in the vicinity of the plate corner, that the concentrated Kirchhoff reaction force in the corner point is equal to zero. However, if even a very small, but finite, minimum thickness is considered in the problem, then the Kirchhoff corner force is finite. Now, plate optimization problems are known to be extremely sensitive with respect to concentrated forces[5,30]; at points of action of such forces, the thickness function will tend to infinity unless a specified maximum constraint, as in the present formulation, constrains the thickness function against such behaviour, *viz.* the plate corner in Fig. 2.
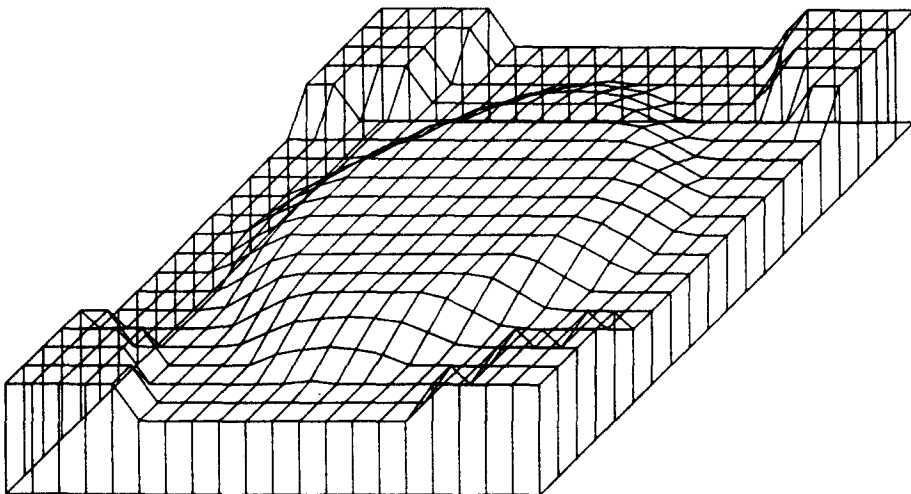

Fig. 1. Simply supported square plate, $h_{max}/h_{min} = 1.5$, $h_u/h_{min} = 1.25$; $\pi/\pi_u = 0.824$. A 10 × 10 grid is used for a quarter of the plate.
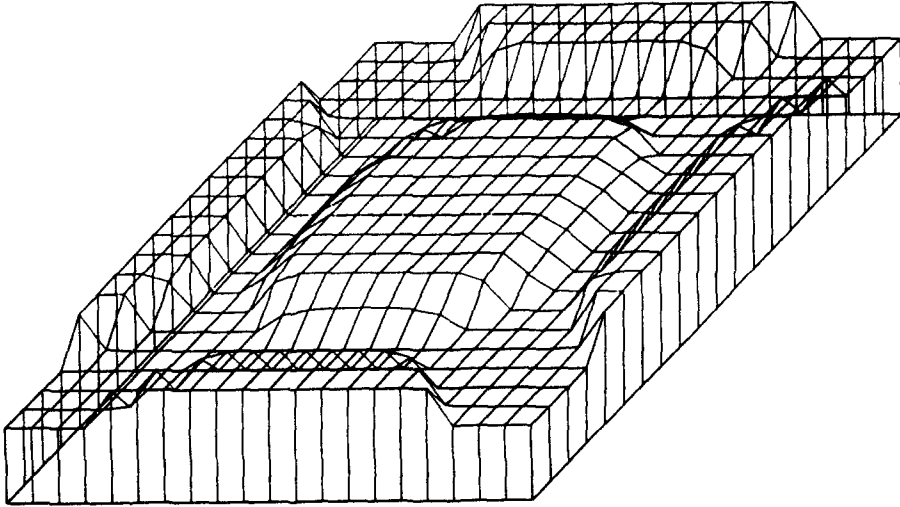
Fig. 2. Clamped square plate, $h_{max}/h_{min} = 1.5$, $h_u/h_{min} = 1.25$; $\pi/\pi_u = 0.707$. A 10×10 grid is used for a quarter of the plate.

The thickness variations shown in Figs. 1 and 2 are qualitatively very similar to those published in Ref. [20], where, however, the numerical procedure seems to be less attractive than the approach developed in the present paper from the point of view of simplicity and effectivity. In Ref. [20], only results associated with the ratio $h_{max}/h_{min} = 1.5$ are presented.

For problems associated with moderate to large h_{max}/h_{min} ratios, we found that different local optimal solutions could be obtained by starting the iterative procedure with different initial thickness functions, keeping all other input and problem data unchanged. Thus, as was found for a similar optimization problem[17], the present problem, too, seems to possess a number of local optimal solutions.

For large h_{max}/h_{min} ratios, we obtain thickness distributions with significant stiffeners as illustrated by the quarter of the calmped plate shown in Fig. 3. This result is associated with $h_u/h_{min} = 2$ and $h_{max}/h_{min} = 6$, and the compliance is found to be 21.8% of the compliance of a corresponding uniform plate. Concerning the stiffeners, we should like to underline that they are formed automatically by the optimization, that is, except for the total plate volume and thickness constraints, no constraints, e.g. conditions concerning location, number or width of the stiffeners, are imposed.

The solution shown in Fig. 3 is associated with the highest integral stiffness (smallest compliance) from among other stationary solutions obtained for the given set of problem data. In fact, the solution is determined by an incremental procedure of "optimal structural remodeling"[31], where a uniform plate of thickness h_{min} is taken as the starting structure, and where fractions of the total plate volume V are successively applied for optimal improvement of the structure obtained from the previous step of remodeling, until the entire available volume V is used. For large h_{max}/h_{min} values and a given plate grid, this approach generally seems to lead directly to the "best" local optimal solution and to demand less computer time than the procedure considered previously, where all the available volume of plate material is applied at one time.
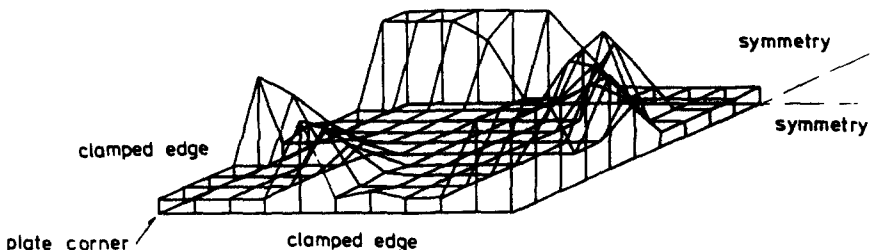

Fig. 3. Quarter of clamped square plate, $h_{max}/h_{min} = 6$, $h_u/h_{min} = 2$; $\pi/\pi_u = 0.218$. A 10×10 grid is used for the quarter plate.

However, the numerical solution for the clamped plate in Fig. 3 cannot be designated as the final answer to the problem considered, because we have found that solutions associated with large h_{max}/h_{min} ratios are significantly dependent on the fineness of the grid used in the numerical solution procedure. The result in Fig. 3 is obtained on the basis of 10×10 equally spaced grid points for one quarter of the plate. If we solve precisely the same problem as in Fig. 3, but use 20×20 equally spaced grid points for the quarter plate, we obtain the result shown in Fig. 4,† where more stiffeners are formed, and where the compliance is now 20.4% of the compliance of the uniform reference plate.

Thus, if finer and finer grids are used, we find decreasing compliances and that more and more stiffeners are formed. These stiffeners become thinner and thinner since V, h_{max} and h_{min} are not changed. Increasing the grid fineness, a possible limiting design could not be obtained within the capacity of our computer and probably cannot be found at all. Thus, the present formulation of the optimization problem does not seem to possess a global optimal solution if h_{max}/h_{min} is large.

5. ANNULAR PLATES

In order to study the fundamental questions concerning the behaviour of numerical solutions and the very formulation of optimization problems for solid plates in greater detail, we shall now use a polar coordinate system r, θ for reasons of convenience that will be apparent in the sequel. Taking $r = x_1$ and $\theta = x_2$, the metric tensor for the plate mid-plane becomes

$$a^{\alpha\beta} = \begin{Bmatrix} 1 & 0 \\ 0 & r^{-2} \end{Bmatrix}, \quad a_\alpha{}^\beta = \begin{Bmatrix} 1 & 0 \\ 0 & 1 \end{Bmatrix}, \quad a_{\alpha\beta} = \begin{Bmatrix} 1 & 0 \\ 0 & r^2 \end{Bmatrix} \tag{26}$$

which implies that from among the Christoffel symbols

$$\begin{Bmatrix} \epsilon \\ \alpha\ \beta \end{Bmatrix} = \frac{1}{2} a^{\epsilon\delta}(a_{\alpha\delta,\beta} + a_{\beta\delta,\alpha} - a_{\alpha\beta,\delta}) \tag{27}$$

only the following will be different from zero,

$$\begin{Bmatrix} 2 \\ 1\ 2 \end{Bmatrix} = \begin{Bmatrix} 2 \\ 2\ 1 \end{Bmatrix} = r^{-1}, \quad \begin{Bmatrix} 1 \\ 2\ 2 \end{Bmatrix} = -r. \tag{28}$$

Using now the general rule for covariant differentiation of tensors, we find that the contravariant, mixed and covariant components of the moment tensor in eqn (2) can be
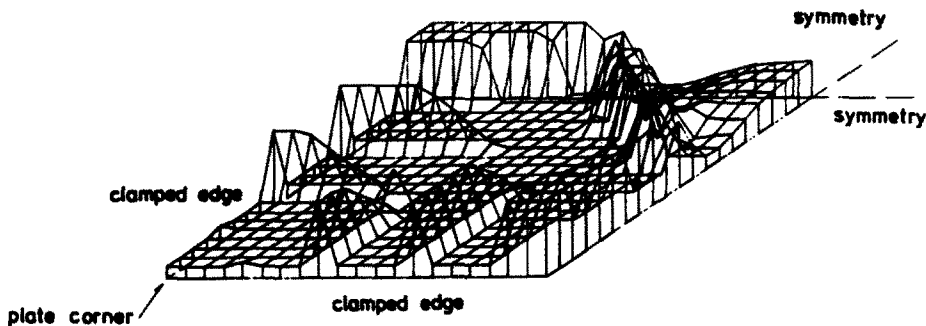

Fig. 4. Quarter of a clamped square plate, $h_{max}/h_{min} = 6$, $h_u/h_{min} = 2$; $\pi/\pi_u = 0.204$. A 20×20 grid is used for the quarter plate.

†It is interesting to note that this result has a remarkable similarity with a result obtained by Prof. Prager[32] for a quite different problem, namely minimum-weight design of rectangular grillages against plastic collapse; the distribution of stiffeners in Fig. 4 of the present paper strongly resembles the optimal beam layout in Fig. 4b of Ref. [32].

expressed in terms of the deflection w and plate rigidity D as follows,

$$M^{11} = M_1{}^1 = M_{11} = D\left(w_{,rr} + \frac{\nu}{r}\,w_{,r} + \frac{\nu}{r^2}\,w_{,\theta\theta}\right)$$

$$M^{22} = r^{-2}M_2{}^2 = r^{-4}M_{22} = Dr^{-2}\left(\nu w_{,rr} + \frac{1}{r}\,w_{,r} + \frac{1}{r^2}\,w_{,\theta\theta}\right)$$

$$M^{12} = M^{21} = M_1{}^2 = r^{-2}M_2{}^1 = r^{-2}M_{12} = r^{-2}M_{21} = (1-\nu)Dr^{-1}\left(\frac{1}{r}\,w_{,\theta}\right)_{,r}. \tag{29}$$

Along a curve $r = \text{const}$, the Kirchhoff shear force in eqn (7) has the form $Q = -M_{,r}^{11} + rM^{22} - r^{-1}M^{11} - 2M_{,\theta}^{12}$ and corresponds physically to the radial (Kirchhoff) shear force Q_r per unit length. By means of (29), this quantity can be expressed by w and D as

$$Q_r = -D_{,r}\left(w_{,rr} + \frac{\nu}{r}\,w_{,r} + \frac{\nu}{r^2}\,w_{,\theta\theta}\right) - D\left(w_{,rr} + \frac{1}{r}\,w_{,r} + \frac{1}{r^2}\,w_{,\theta\theta}\right)_{,r}$$

$$-(1-\nu)D\frac{1}{r}\left(\frac{1}{r}\,w_{,\theta\theta}\right)_{,r} - 2(1-\nu)D_{,\theta}\frac{1}{r}\left(\frac{1}{r}\,w_{,\theta}\right)_{,r}. \tag{30}$$

The physical moment components, i.e. radial bending moment M_{rr}, tangential bending moment $M_{\theta\theta}$ and twisting moment $M_{r\theta} = M_{\theta r}$ (all per unit length) are defined as follows in terms of the mixed moment tensor components, and can be expressed by w and D as

$$M_{rr} = M_1{}^1 = D\left(w_{,rr} + \frac{\nu}{r}\,w_{,r} + \frac{\nu}{r^2}\,w_{,\theta\theta}\right), \quad M_{\theta\theta} = M_2{}^2 = D\left(\nu w_{,rr} + \frac{1}{r}\,w_{,r} + \frac{1}{r^2}\,w_{,\theta\theta}\right),$$

$$M_{r\theta} = M_{\theta r} = \sqrt{(M_1{}^2 M_2{}^1)} = (1-\nu)D\left(\frac{1}{r}\,w_{,\theta}\right)_{,r}. \tag{31}$$

Via eqns (29), the function g in eqn (18) is seen to take the following form in terms of the physical moments,

$$g(x^\alpha) = (M_{rr} + M_{\theta\theta})^2 + 2(1+\nu)[M_{r\theta}^2 - M_{rr}M_{\theta\theta}]. \tag{32}$$

By means of eqns (26)–(32) it would now be a simple task to specialize the governing tensor equations for our plate optimization problem to a general description in polar coordinates, but this will be omitted here.

Instead, we shall from now on assume that the plate is rotationally symmetric, i.e. that its thickness h and bending rigidity D depend only on the distance r from the symmetry axis, implying $h = h(r)$ and $D = D(r)$. Furthermore, we shall limit outselves to considering load distribution functions $p(r, \theta)$ of the special type

$$p(r, \theta) = f(r)\cos n\theta, \tag{33}$$

where f is a given function that only depends on r and where n is a given integer. Equation (33) thus models a rotationally symmetric load distribution for $n = 0$, whereas eqn (33) for $n \neq 0$ models a load $p(r, \theta)$ that has the trace $f(r)$ for $\theta = 0$ and varies harmonically with θ in the circumferential direction. Assuming the boundary conditions to be homogeneous, the plate deflection function $w(r, \theta)$ then has the simple form

$$w(r, \theta) = u(r)\cos n\theta. \tag{34}$$

The assumptions introduced here offer the mathematical simplification that the governing non-linear partial differential equations of our optimization problem reduce to ordinary differential equations after a separation of variables and this means in turn that much less computer space and time are required for the numerical solution procedure. These sim-

plifications do not impede our further study of plate stiffener formation; the rotationally symmetric plate possesses the possibility of increasing its stiffness against circumferentially varying loads $p(r, \theta)$ by forming concentric, circumferential stiffeners that may effectively counteract the circumferential curvatures of the deflection function $w(r, \theta)$.

Now, substituting (29) with w given by (34) into the equilibrium eqn (1), $\cos n\theta$ factors out and we obtain an ordinary differential equation for the plate rigidity function $D(r)$ and the θ-independent part $u(r)$ of the deflection function. After some manipulation, this equation can be written in the comparatively compact form

$$\left\{ r\left[D\left(u'' + \frac{1}{r}u' - \frac{n^2}{r^2}u \right)' + D'\left(u'' + \frac{\nu}{r}u' - \frac{\nu n^2}{r^2}u \right) \right] \right\}' - D\frac{n^2}{r}\left(u'' + \frac{1}{r}u' - \frac{n^2}{r^2}u \right)$$

$$- (1 - \nu)D'n^2\left(\frac{1}{r}u \right)' = f(r)r, \tag{35}$$

where primes denote differentiation with respect to r. Equation (35) replaces eqn (4) in the formulation of our new optimization problem.

For deflection functions in the form (34), the stress resultants in eqns (30) and (31) reduce to

$$Q_r = q_r \cos n\theta, \quad M_{rr} = m_{rr} \cos n\theta, \quad M_{\theta\theta} = m_{\theta\theta} \cos n\theta, \quad M_{r\theta} = m_{r\theta} \sin n\theta, \tag{36}$$

respectively, where the θ-independent parts of the stress resultants are given by

$$q_r = -D'\left(u'' + \frac{\nu}{r}u' - \frac{\nu n^2}{r^2}u \right) - D\left(u'' + \frac{1}{r}u' - \frac{n^2}{r^2}u \right)' + (1 - \nu)D\frac{n^2}{r}\left(\frac{1}{r}u \right)'$$

$$m_{rr} = D\left(u'' + \frac{\nu}{r}u' - \frac{\nu n^2}{r^2}u \right), \quad m_{\theta\theta} = D\left(\nu u'' + \frac{1}{r}u' - \frac{n^2}{r^2}u \right), \quad m_{r\theta} = -(1 - \nu)D\left(\frac{n}{r}u \right)', \tag{37}$$

respectively.

In order to establish the optimality condition, we now substitute eqn (31), with M_{rr}, $M_{\theta\theta}$ and $M_{r\theta}$ given by eqns (36), into (A20) and perform a separate integration over θ in the interval $0 \le \theta \le 2\pi$, thereby ruling out θ-dependence. Upon applying the usual argument from the calculus of variations, using eqn (3) and scaling Lagrangian multipliers Λ, λ and κ, we obtain the optimality condition in the form

$$h^{-4}[(m_{rr} + m_{\theta\theta})^2 + 2(1 + \nu)(m_{r\theta}^2 - m_{rr}m_{\theta\theta})] = \Lambda - \lambda + \kappa \tag{38}$$

which takes the place of eqn (15) for the present problem.

Defining the function g as

$$g(r) = (m_{rr} + m_{\theta\theta})^2 + 2(1 + \nu)(m_{r\theta}^2 - m_{rr}m_{\theta\theta}), \tag{39}$$

from now on, we instead of eqn (19) obtain the formula

$$h(r) = \begin{cases} h_{\max} & \text{if} \quad (g(r)/\Lambda)^{1/4} \ge h_{\max}, \quad r \in r_{ca} \\ (g(r)/\Lambda)^{1/4}, \quad r \in r_u \\ h_{\min} & \text{if} \quad (g(r)/\Lambda)^{1/4} \le h_{\min}, \quad r \in r_{cb} \end{cases} \tag{40}$$

for the optimal, symmetrical plate thickness function $h(r)$. Here, r_{ca}, r_u and r_{cb} denote the unions of sub-intervals for the radial distance r, where the plate thickness is constrained from above, unconstrained and constrained from below, respectively.

Finally, substituting eqn (40) into eqn (9) and solving for Λ, we obtain the formula

$$\Lambda = \left[\frac{\displaystyle\int_{r_u} g(r)^{1/4} r \, dr}{\dfrac{V}{2\pi} - h_{\min} \displaystyle\int_{r_{cb}} r \, dr - h_{\max} \displaystyle\int_{r_{ca}} r \, dr} \right]^4 , \tag{41}$$

which takes the place of eqn (20) for our new problem.

As objects of optimization, we now consider annular plates with various combinations of boundary conditions at their inner and outer circular edges. In accordance with eqns (5a–c) we deal with simply supported, clamped and free plate edges, and in the present notation corresponding boundary conditions can be expressed as

$$u(r^*) = 0, \quad m_{rr}(r^*) = 0 \tag{42a}$$

$$u(r^*) = 0, \quad u'(r^*) = 0 \tag{42b}$$

$$m_{rr}(r^*) = 0, \quad q_r(r^*) = 0, \tag{42c}$$

respectively, where q_r and m_{rr} are given in terms of u and D by eqns (37) and where r^* denotes the radius of the inner or the outer plate edge.

In the iterative solution procedure of Section 2, where u now replaces w, we in Step II solve the present version (35) of the plate equilibrium equation (4) by means of the finite element method, sub-dividing the distance between the inner and outer plate edges by means of a number of equally spaced nodal points, where the deflection u and slope u' are used as the nodal unknowns, and where continuity is imposed on these quantities. Each element between two adjacent nodal points has a constant thickness and its shape function for the deflection u is taken to be a complete third order polynomium. This approach is chosen because the different boundary conditions (42a–c) are easily imposed, and because it admits thickness jumps between neighbouring elements, which is a behaviour the plate may tend to exhibit.

When the deflection function $u(r)$ is determined in Step II, we in Step III compute m_{rr}, $m_{\theta\theta}$ and $m_{r\theta}$ by means of eqns (37) and the function $g(r)$ by eqn (39). In Step IV, Λ is then determined by eqn (41). The computation of the new values of the constant thicknesses of the elements in Step IV is performed by means of eqn (40) on the basis of determining for each element sub-interval a constant, properly averaged value of the function g in eqn (39).

Results and discussion

We now present a number of numerical results obtained for annular plates acted on by load distributions (33) with f constant and n a given integer. In all the examples, the inner plate radius is taken to be one-fifth of the outer radius, the ratio between the thickness constraints is $h_{\max}/h_{\min} = 5$, and the total plate volume is given via the ratio $h_u/h_{\min} = 1.6579$, where h_u is the plate thickness corresponding to a uniform distribution of the available volume over the plate area. Poisson's ratio of the plate material is taken to be $\nu = 0.25$. In the following we state the compliance π of an optimized plate as a fraction of the compliance π_u of a corresponding uniform plate that has the same loading, boundary conditions, total volume and inner and outer plate radii and that is made of the same material.

Figures 5(a)–(i) illustrate numerical solutions for annular plates with the nine possible combinations of clamped, simply supported and free inner and outer plate edges. Each solution is illustrated by a radial section through the plate, together with the θ-independent part $u(r)$ of the deflection function. All the results are associated with the load wave number $n = 4$ and 100 elements are used in the numerical procedure. It is noted that circumferential stiffeners are formed in all the plates, and it is also interesting that some of the plates with simply supported and free edges build up ring-shaped edge reinforcements that reduce the slope of the deflection.

To investigate the influence of the load wave number n on the numerical results, we take the clamped-clamped plate as an example and first optimize it subject to $n = 6$ and 10, respectively, again using 100 elements. The results are shown in Figs. 6(a)–(b), and may be compared with the result for $n = 4$ in Fig. 5(a). As is to be expected, the number of stiffeners tends to increase
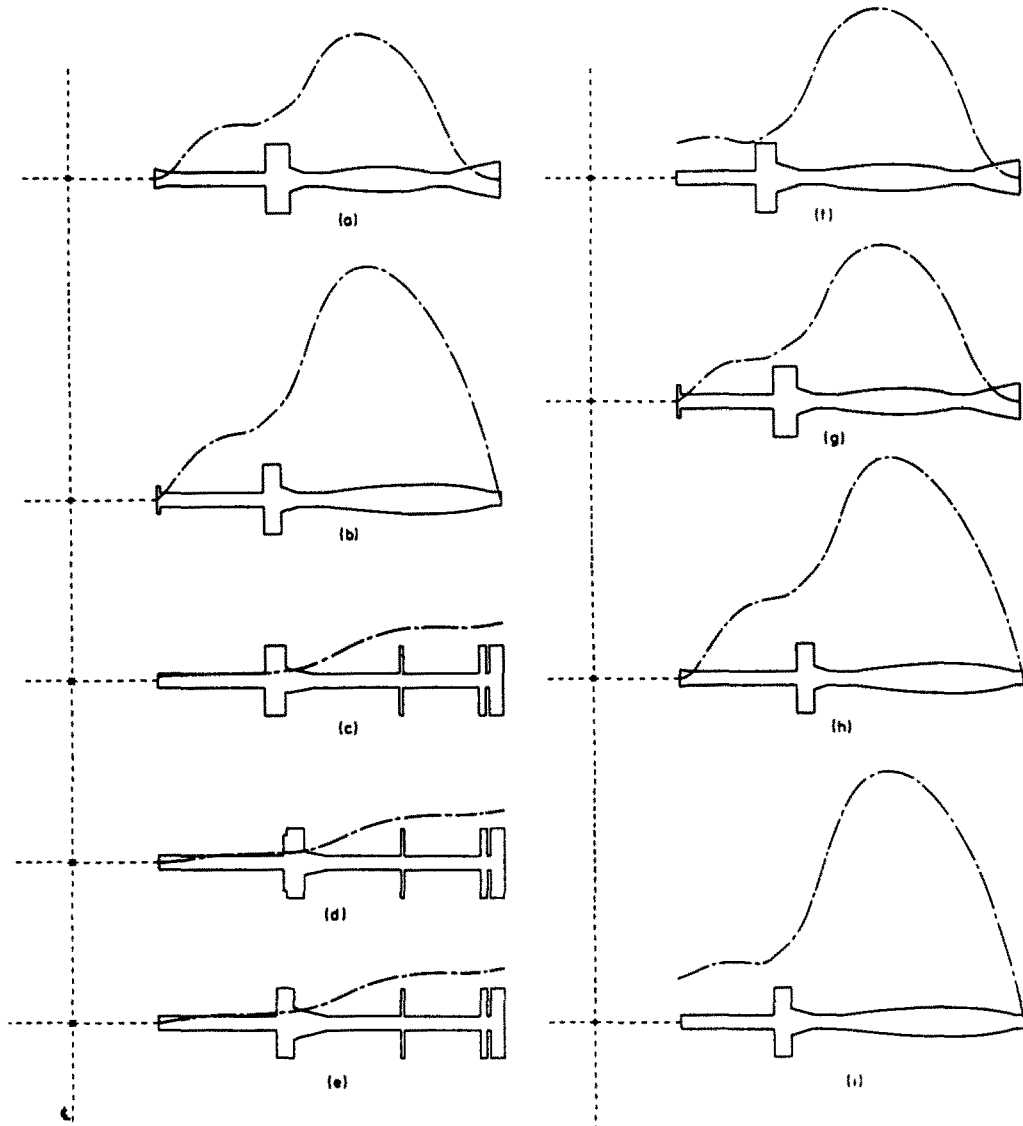
Fig. 5. Results of optimizing annular plates of different boundary conditions. Solid curves show radial sections through the plates and dashed-dotted lines indicate the r-independent part u of the deflection functions. The load and deflection wave number n in the circumferential direction is equal to 4 in each example. The inner plate radius is one-fifth of the outer radius and the results are based on subdividing the plates into 100 elements. (a) Clamped-clamped plate, $\pi/\pi_u = 0.536$. (b) Simply supported-simply supported plate, $\pi/\pi_u = 0.605$. (c) Free-free plate, $\pi/\pi_u = 0.265$. (d) Clamped-free plate, $\pi/\pi_u = 0.251$. (e) Simply supported-free plate, $\pi/\pi_u = 0.256$. (f) Free-clamped plate, $\pi/\pi_u = 0.617$. (g) Simply supported-clamped plate, $\pi/\pi_u = 0.564$. (h) Clamped-simply supported plate, $\pi/\pi_u = 0.584$. (i) Free-simply supported plate, $\pi/\pi_u = 0.645$.

with increasing n. Optimizing a clamped-clamped plate for $n = 0$, 1 and 2, respectively, see Figs. 7(a)–(c), none of our numerical results exhibits stiffener-like behaviour even though we increase the number of elements to 300, thereby favouring formation of possible stiffeners, which should be expected in view of [3].

Let us now investigate how the number of elements used affects the results, taking the clamped-clamped plate associated with $n = 4$ as an example. Figures 8(a)–(d) show the results obtained by using 150, 200, 250 and 300 elements, respectively, to cover the interval of the radial distance from the inner to the outer plate radius. Figures 8(a)–(d) illustrate that the number of stiffeners increases rapidly and that the compliance decreases as the number of elements is increased. Moreover, the stiffeners are seen to become thinner and thinner as the number of elements increases, the widths of most of them in fact being equal to the width of one element only.
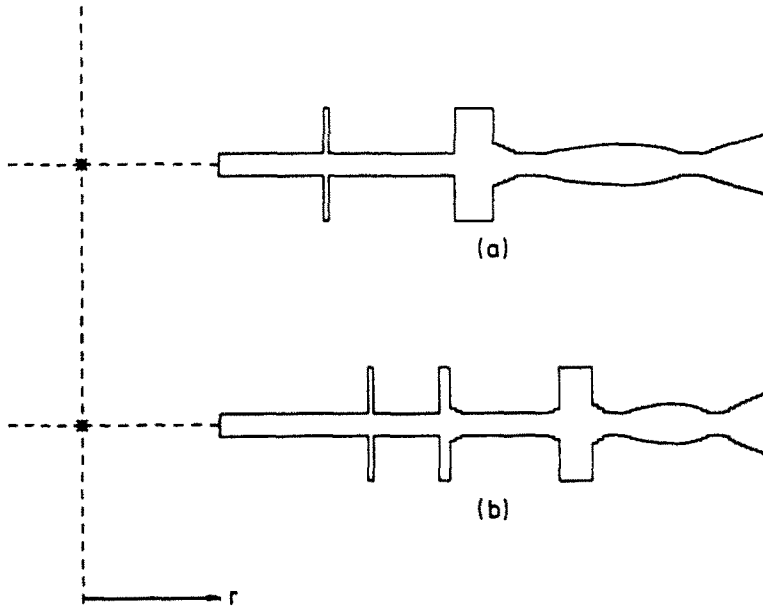
Fig. 6. Doubly clamped annular plates optimized for different load wave numbers n: (a) $n = 6$, $\pi/\pi_u =$ 0.491. (b) $n = 10$, $\pi/\pi_u = 0.408$. The plates are subdivided into 100 elements.
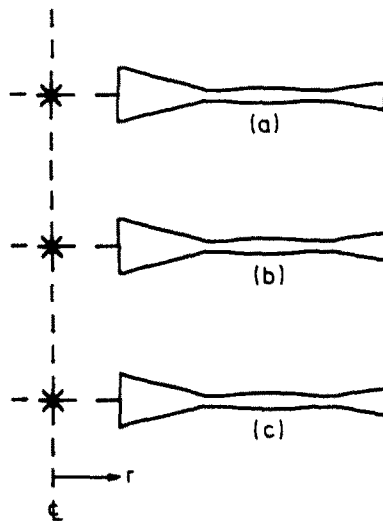

Fig. 7. Doubly clamped annular plates optimized for small load wave numbers n. (a) $n = 0$, $\pi/\pi_u = 0.463$. (b) $n = 1$, $\pi/\pi_u = 0.489$. (c) $n = 2$, $\pi/\pi_u = 0.589$. The plates are subdivided into 300 elements.

These results clearly indicate that no limiting solution will be found if we continuously increase the number of elements, and this implies that there is no global optimal solution to the present formulation of our optimization problem for sufficiently large values of the ratio h_{max}/h_{min}.

Optimization with segmentwise constant thickness and a minimum stiffener width constraint

From the results reported above, the natural question arises of whether an optimization problem associated with a large h_{max}/h_{min} ratio will possess a global optimal solution if, in addition to the minimum and maximum thickness constraints, we consider a minimum allowable width of possible stiffeners in the mathematical formulation of the problem.

To study this question, we impose the condition that the thickness function may not vary within plate segments consisting of a given number of adjacent finite elements. We then solve the problem a number of times where different numbers of elements are used, but where the proportion between the number of elements within the segments of constant thickness and the
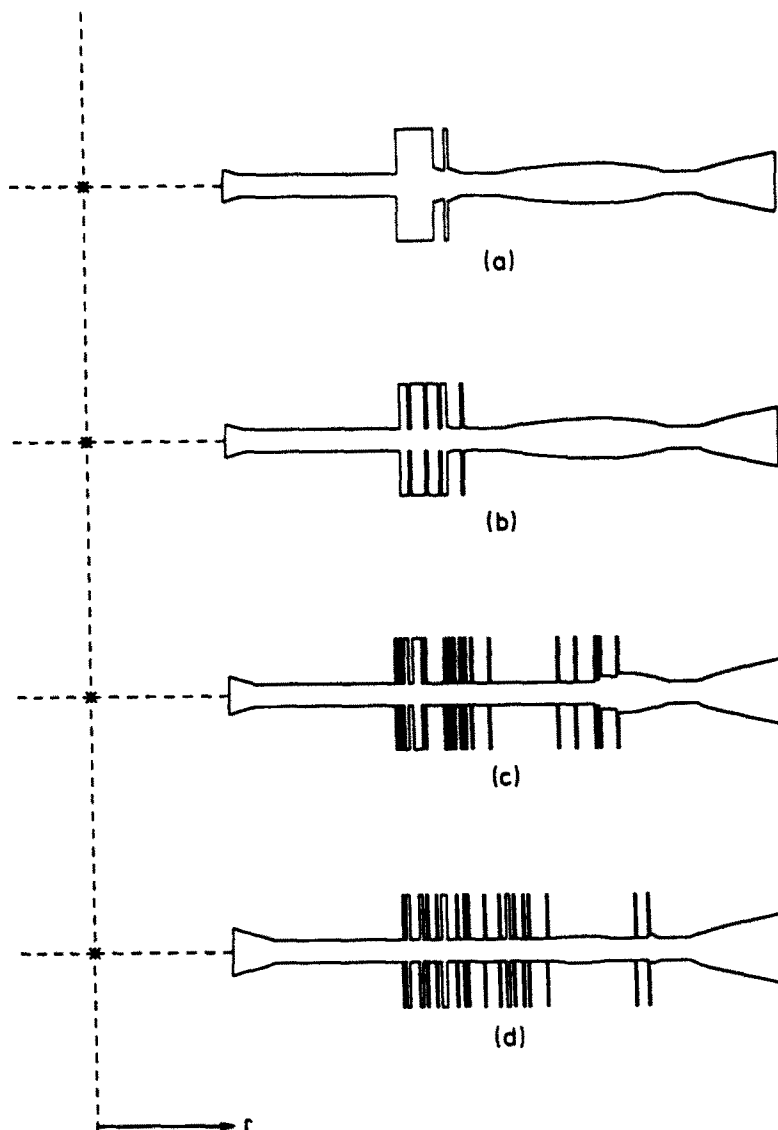
Fig. 8. The dependence of the design of a doubly clamped annular plate with $n = 4$ on the number of elements used. (a) 150 elements, $\pi/\pi_u = 0.536$. (b) 200 elements, $\pi/\pi_u = 0.525$. (c) 250 elements, $\pi/\pi_u = 0.433$. (d) 300 elements, $\pi/\pi_u = 0.428$.

total number of plate elements is maintained, such that the absolute values of the radial distances of the plate segments are the same in each calculation.

We find that problems associated with a sufficiently large minimum width constraint for possible stiffeners seem to have a global optimal solution, because the same plate design is obtained independently of the starting design and the number of elements used. If a small minimum width constraint is specified, however, the results are less conclusive since different local optimal designs can be obtained by starting out from different initial designs and using different numbers of elements.

6. CONCLUDING REMARKS

Some fundamental questions concerning the mathematical formulation for optimal design of plates on the basis of thin plate theory, are investigated in this paper. Our numerical results show that the geometrically constrained formulation considered, significantly prompts the formation of plate stiffeners. However, as in a geometrically unconstrained formulation investigated in [17], we find that a number of local optimal solutions exist and that a possible global optimal plate thickness function does neither exist in the class of smooth functions nor in the class of smooth functions with a finite number of discontinuities. Similar results are to be

expected for corresponding formulations of optimal plate design with respect to minimizing the largest deflection, maximizing the fundamental vibration frequency, buckling load, etc.

The current results indicate clearly that the global optimal design is a plate which, at least in some regions, is equipped with an infinite number of infinitely thin stiffeners. Indeed, this has been confirmed by follow-up research[33, 34] on axisymmetric annular plates. In Refs. [33, 34], which deal with static compliance and transverse vibration frequency design, respectively, new optimal design formulations have been developed on the basis of a revised plate model where the density of infinitely thin stiffeners is used as the design variable and where the plate bending rigidity becomes an orthotropic function of the stiffener density.

REFERENCES

1. Z. Mróz, Multi-parameter optimal design of plates and shells. *J. Struct. Mech.* 1, 371–392 (1973).
2. K. A. Lur'e and A. V. Cherkaev, Prager theorem application to optimal design of thin plates (in Russian). *MTT Mechanics of Solids* 11, 157–159 (1976).
3. R. Reiss, Optimal conpliance criterion for axisymmetric solid plates, *Int. J. Solids Structures* 12, 319–329 (1976).
4. N. C. Huang, Optimal design of elastic structures for maximum stiffness. *Int. J. Solids Structures* 4, 689–700 (1968).
5. N. Olhoff, Optimal design of vibrating circular plates. *Int. J. Solids Structures* 6, 139–156 (1970).
6. J. C. Frauenthal, Constrained optimal design of circular plates against buckling. *J. Struct. Mech.* 1, 159–186 (1972).
7. N. Olhoff, Optimal design of vibrating rectangular plates. *Int. J. Solids Structures* 10, 93–109 (1974).
8. N. M. Gura and A. P. Seyranian, Optimum circular plate with constraints on the rigidity and frequency of natural oscillations (in Russian). *MTT Mechanics of Solids* 12, 138–145 (1977).
9. G. J. Simitses, Optimal vs stiffened circular plate. *AIAA J.* 11, 1409–1410 (1973).
10. J.-L. Armand, Numerical solutions in optimization of structural elements. *Paper at 1st. Int. Conf. on Computational Methods in Nonlinear Mech.* Austin, Texas, U.S.A. (Sept. 1974).
11. J.-L. Armand and B. Lodier, Optimal design of bending elements. *Int. J. Num. Meth. Engng* 13, 373–384 (1978).
12. W. A. Nash, Effect of a concentric reinforcing ring on stiffness and strength of a circular plate. *J. Appl. Mech.* 15, 25–29 (1949).
13. G. J. Megarefs, Method of minimal weight design of axisymmetric plates. *Proc. ASCE* 92, EM6, 79–99 (1966).
14. J. F. Brotchie, Method for minimal design of axisymmetric plates. *Proc. ASCE* 93, EM5, 173–175 (1967).
15. W. Kozlowski and Z. Mróz, Optimal design of solid plates. *Int. J. Solids Structures* 5, 781–794 (1969).
16. A. M. Samsonov, Optimum location of thin elastic rib on elastic plate (in Russian). *MTT Mechanics of Solids* 13, 132–138 (1978).
17. N. Olhoff, On singularities, local optima and formation of stiffeners in optimal design of plates. *Proc. IUTAM Symp. on Optimization in Structural Design* (Edited by A. Sawczuk and Z. Mróz), Warsaw, pp. 82–103. Springer-Verlag, Berlin (1975).
18. A. P. Seyranian, A study of an extremum in the optimal problem of a vibrating circular plate (in Russian). *MTT Mechanics of Solids* 13, 113–118 (1978).
19. N. V. Banichuk, Optimal plate shapes in bending problems (in Russian). *MTT Mechanics of Solids* 10, 180–188 (1975).
20. N. V. Banichuk, V. M. Kartvelishvili and A. A. Mironov, Numerical solution of two-dimensional optimization problems for elastic plates (in Russian). *MTT Mechanics of Solids* 12, 68–78 (1977).
21. N. V. Banichuk, V. M. Kartvelishvili and A. A. Mironov, Optimization problems with local performance criteria in the theory of plate bending (in Russian). *MTT Mechanics of Solids* 13, 124–131 (1978).
22. E. F. Masur, Optimality in the presence of discreteness and discontinuity. *Proc. IUTAM Symp. on Optimization in Structural Design* (Edited by A. Sawczuk and Z. Mróz), Warsaw, pp. 441–453. Springer-Verlag, Berlin (1975).
23. G. A. Hegemier and H. T. Tang, A variational principle, the finite element method and optimal structural design for given deflection. *Proc. IUTAM Symp. on Optimization in Structural Design* (Edited by A. Sawczuk and Z. Mróz), Warsaw, pp. 464–483. Springer-Verlag, Berlin (1975).
24. W. Prager and J. E. Taylor, Problems of optimal structural design. *J. Appl. Mech.* 35, 102–106 (1968).
25. J. E. Taylor, On the prediction of structural layout for maximum stiffness. *J. Optimization Th. Appl.* 15, 145–155 (1975).
26. E. F. Masur, Optimum stiffness and strength of elastic structures. *ASCE* 96, EM5, 621–640 (1970).
27. W. Flügge, *Tensor Analysis and Continuum Mechanics.* Springer-Verlag, Berlin (1972).
28. F. Niordson, *Introduction to Shell Theory,* Dept. of Solid Mechanics, The Technical University of Denmark (1980).
29. S. Timoshenko and S. Woinowsky-Krieger, *Theory of Plates and Shells.* McGraw-Hill, New York (1959).
30. S. Lukasiewicz, *Local Loads in Plates and Shells.* Noordhoff, Amsterdam (1979).
31. N. Olhoff and J. E. Taylor, On optimal structural remodeling. *J. Optimization Th. Appl.* 27, 571–582 (1979).
32. W. Prager, Optimal arrangement of the beams of a rectangular grillage. In *Problemi Attuali di Meccanica e Applicata,* pp. 239–249. Accademia delle Scienze, Torino (1977).
33. K.-T. Cheng, On some new optimal design formulations for plates. *DCAMM Rept.* No. 189, The Danish Center for Applied Mathematics and Mechanics (1980).
34. N. Olhoff, K. A. Lurie, A. V. Cherkaev and A. V. Fedorov, Sliding regimes and anisotropy in optimal design of vibrating axisymmetric plates. *DCAMM Rept.* No. 192, The Danish Center for Applied Mathematics and Mechanics (1980).

APPENDIX

In this section, we shall derive in some detail the Euler–Lagrange equations expressing the conditions of stationarity of the functional π^* in eqn (12) with respect to arbitrary admissible variations of the deflection w and the plate thickness h, respectively.

Variation of w yields the stationarity condition

$$-\int_\Omega p\delta w \, d\Omega + \int_\Omega \eta d_\alpha d_\beta \delta M^{\alpha\beta}(w) \, d\Omega = 0, \tag{A1}$$

where the expression of $M^{\alpha\beta}$ in terms of w is given by eqn (2). Using the identity

$$\eta d_\alpha d_\beta \delta M^{\alpha\beta} = d_\alpha(\eta d_\beta \delta M^{\alpha\beta}) - (d_\alpha \eta)(d_\beta \delta M^{\alpha\beta})$$

to replace the second integral in (A1) by two new integrals and applying the divergence theorem to the first of them, we get

$$-\int_\Omega p\delta w \, d\Omega + \oint_\omega n_\alpha \eta d_\beta \delta M^{\alpha\beta}(w) \, d\omega - \int_\Omega \{d_\alpha \eta\}\{d_\beta \delta M^{\alpha\beta}(w)\} \, d\Omega = 0, \tag{A2}$$

where ω is the boundary curve of the domain Ω and n_α is the outward unit normal vector in the x^α plane to this curve.

An analogous treatment of the last term on the r.h.s. of eqn (A2) gives the equation

$$-\int_\Omega p\delta w \, d\Omega + \oint_\omega n_\alpha \eta d_\beta \delta M^{\alpha\beta}(w) \, d\omega - \oint_\omega \delta M^{\alpha\beta}(w)n_\beta d_\alpha \eta \, d\omega + \int_\Omega \delta M^{\alpha\beta}(w)d_\alpha d_\beta \eta \, d\Omega = 0. \tag{A3}$$

In the third integral of eqn (A3) we now put $d_\alpha \eta = \psi n_\alpha + \zeta t_\alpha$, where t_α is the unit tangent vector to ω and where ψ and ζ denote the scalar slopes of the function η in the normal and tangential directions, respectively, to the curve ω. Using then the identity

$$\zeta \delta M^{\alpha\beta}(w)t_\alpha n_\beta = \frac{\partial(\eta \delta M^{\alpha\beta}(w)t_\alpha n_\beta)}{\partial \omega} - \eta \frac{\partial(\delta M^{\alpha\beta}(w)t_\alpha n_\beta)}{\partial \omega},$$

and noting that $\zeta = \partial \eta/\partial \omega$, we can write eqn (A3) in the form

$$-\int_\Omega p\delta w \, d\Omega + \oint_\omega \eta \left\{ n_\alpha d_\beta \delta M^{\alpha\beta}(w) + \frac{\partial(\delta M^{\alpha\beta}(w)t_\alpha n_\beta)}{\partial \omega} \right\} d\omega - \oint_\omega \frac{\partial(\eta \delta M^{\alpha\beta}(w)t_\alpha n_\beta)}{\partial \omega} \, d\omega$$
$$- \oint_\omega \psi(\eta)\delta M^{\alpha\beta}(w)n_\alpha n_\beta \, d\omega + \int_\Omega \delta M^{\alpha\beta}(w)d_\alpha d_\beta \eta \, d\Omega = 0. \tag{A4}$$

Here, the Kirchhoff shear force $Q(w)$ given by eqn (7) and the effective bending moment $M_B(w)$ given by eqn (6) can be introduced in the first and third curve integrals, respectively. Since the curve ω is closed, the second curve integral will vanish if ω is smooth, but if ω has one or more corner points x_i^α, $i = 1,2,\ldots$, where the vectors t_α and n_β change discontinuously from t_α^- and n_β^- to t_α^+ and n_β^+, respectively, the second curve integral will become equal to

$$-\sum_i \{\eta \delta Q^*(w)\}_{x^\alpha = x_i^\alpha},$$

where

$$\{Q^*\}_{x^\alpha = x_i^\alpha} = \{M^{\alpha\beta}t_\alpha^+ n_\beta^+ - M^{\alpha\beta}t_\alpha^- n_\beta^-\}_{x^\alpha = x_i^\alpha} \tag{A5}$$

identifies the concentrated Kirchhoff force at a possible corner point x_i^α. Hence, we can write eqn (A4) as

$$-\int_\Omega p\delta w \, d\Omega - \oint_\omega \eta \delta Q(w) \, d\omega + \sum_i \{\eta \delta Q^*(w)\}_{x^\alpha = x_i^\alpha} - \oint_\omega \psi(\eta)\delta M_B(w) \, d\omega + \int_\Omega \delta M^{\alpha\beta}(w)d_\alpha d_\beta \eta \, d\Omega = 0. \tag{A6}$$

Let us now address our attention to the last integral on the l.h.s. of eqn (A6). Using the shorter notation δI for this integral,

$$\delta I = \int_\Omega \delta M^{\alpha\beta}(w)d_\alpha d_\beta \eta \, d\Omega, \tag{A7}$$

and introducing covariant differentiation throughout in the expression for $M^{\alpha\beta}$ in eqn (2), we have

$$M^{\alpha\beta}(w) = DA^{\sigma\tau\beta\kappa}d_\tau d_\kappa w, \tag{A8}$$

where the fourth order metric tensor $A^{\sigma\tau\beta\kappa}$ is defined by

$$A^{\sigma\tau\beta\kappa} = (1-\nu)a^{\sigma\tau}a^{\beta\kappa} + \nu a^{\alpha\beta}a^{\tau\kappa}. \tag{A9}$$

Equation (A7) can then be written as

$$\delta I = \int_\Omega DA^{\sigma\tau\beta\kappa}\{d_\tau d_\kappa \delta w\}d_\alpha d_\beta \eta \, d\Omega, \tag{A10}$$

but since the tensor $A^{\alpha\gamma\beta\kappa}$ in eqn (A9) possesses the symmetry property $A^{\alpha\gamma\beta\kappa} = A^{\gamma\alpha\kappa\beta}$ due to symmetry of the metric tensor $a^{\alpha\beta}$, it follows from eqn (A8), when this equation is expressed in terms of η, that eqn (A10) can be written in the form

$$\delta I = \int_\Omega M^{\alpha\beta}(\eta) d_\alpha d_\beta \delta w \, d\Omega, \tag{A11}$$

where the moment tensor is now based upon the function η.

Using the identity

$$M^{\alpha\beta}(\eta) d_\alpha d_\beta \delta w = d_\alpha \{ M^{\alpha\beta}(\eta) d_\beta \delta w \} - d_\beta \{ \delta w d_\alpha M^{\alpha\beta}(\eta) \} + \delta w d_\alpha d_\beta M^{\alpha\beta}(\eta)$$

to replace the integral (A11) by three integrals, applying the divergence theorem to the first two of them, we write $d_\beta \delta w = n_\beta \delta \psi + t_\beta \delta \xi$ where ψ and ξ denote the scalar slopes of w in the directions normal and tangential to the curve ω, respectively. Then, upon noting that $\xi = \partial w/\partial \omega$ and using the identity

$$M^{\alpha\beta}(\eta) t_\beta n_\alpha \delta \xi = \frac{\partial(M^{\alpha\beta}(\eta) t_\beta n_\alpha \delta w)}{\partial \omega} - \frac{\partial(M^{\alpha\beta}(\eta) t_\beta n_\alpha)}{\partial \omega} \delta w$$

we obtain the following expression for the integral δI,

$$\delta I = \oint_\omega M^{\alpha\beta}(\eta) n_\alpha n_\beta \delta \psi(w) \, d\omega + \oint_\omega \frac{\partial(M^{\alpha\beta}(\eta) t_\beta n_\alpha \delta w)}{\partial \omega} \, d\omega - \oint_\omega \left\{ n_\beta d_\alpha M^{\alpha\beta}(\eta) + \frac{\partial(M^{\alpha\beta}(\eta) t_\beta n_\alpha)}{\partial \omega} \right\} \delta w \, d\omega$$

$$+ \int_\Omega \{ d_\alpha d_\beta M^{\alpha\beta}(\eta) \} \delta w \, d\Omega. \tag{A12}$$

Since $M^{\alpha\beta}$ is symmetric, it is now possible to introduce in the first and third integrals the effective bending moment $M_B(\eta)$ and Kirchhoff shear force $Q(\eta)$ based on η by means of eqns (6) and (7). Furthermore, the second integral of eqn (A12) vanishes if the curve ω is smooth, but equals

$$- \sum_i \{ Q^*(\eta) \delta w \}_{x^\alpha = x_i^\alpha},$$

where Q^* is defined in eqn (A5), if the curve ω has corner points x_i^α. Consequently, we can write eqn (A12) in the form

$$\delta I = \oint_\omega M_B(\eta) \delta \psi(w) \, d\omega + \oint_\omega Q(\eta) \delta w \, d\omega - \sum_i \{ Q^*(\eta) \delta w \}_{x^\alpha = x_i^\alpha} + \int_\Omega \{ d_\alpha d_\beta M^{\alpha\beta}(\eta) \} \delta w \, d\Omega. \tag{A13}$$

Now, substituting this expression for δI into eqn (A6) via eqn (A7) and collecting terms, we have the variational equation

$$- \oint_\omega \eta \delta Q(w) \, d\omega + \sum_i \{ \eta \delta Q^*(w) \}_{x^\alpha = x_i^\alpha} - \oint_\omega \psi(\eta) \delta M_B(w) \, d\omega + \oint_\omega Q(\eta) \delta w \, d\omega - \sum_i \{ Q^*(\eta) \delta w \}_{x^\alpha = x_i^\alpha}$$

$$+ \oint_\omega M_B(\eta) \delta \Psi(w) \, d\omega + \int_\Omega \{ d_\alpha d_\beta M^{\alpha\beta}(\eta) - p \} \delta w \, d\Omega = 0, \tag{A14}$$

which expresses the stationarity of π^*, eqn (12), for arbitrary admissible variation of w. To be admissible, w must satisfy the boundary conditions (5a), (5b) or (5c) for a particular problem.

Since δw is arbitrary, it follows from eqn (A14), taking eqn (2) into account, that the function $\eta(x^\alpha)$ must satisfy the partial differential equation

$$d_\alpha d_\beta [D\{(1 - \nu) d^\alpha d^\beta \eta + \nu a^{\alpha\beta} d_\gamma d^\gamma \eta \}] = p \tag{A15}$$

in the domain Ω, but this is the same differential equation as governs the deflection $w(x^\alpha)$, see eqn (4). Moreover, it follows from eqn (A14) that, at the plate boundary ω, (i) the function $\eta(x^\alpha)$ must vanish if the distributed Kirchhoff shear force $Q(w)$ of eqn (7) and concentrated Kirchhoff forces $Q^*(w)$ of eqn (A5) at possible corner points x_i^α are not specified, (ii) that the slope $\psi(\eta) = n^\alpha d_\alpha \eta$ of the function η normal to ω must vanish if the effective bending moment $M_B(w)$ in eqn (6) is not specified, (iii) that $Q(\eta)$ and $Q^*(\eta)$ must vanish if the deflection w is not specified and (iv) that $M_B(\eta)$ must vanish if the slope $\Psi(w) = n^\alpha d_\alpha w$ of the deflection w normal to ω is unspecified. All these results clearly imply that the function $\eta(x^\alpha)$ must satisfy the same particular set of boundary conditions (5a), (5b) or (5c) as is specified for the deflection function $w(x^\alpha)$ in a given problem.

Since the functions $\eta(x^\alpha)$ and $w(x^\alpha)$ are governed by the same differential equation and the same set of complete boundary conditions for a particular problem, they must be identical,

$$\eta(x^\alpha) \equiv w(x^\alpha). \tag{A16}$$

It is noted that this result is closely connected with the fact that the differential operator on the l.h.s. of eqn (4) is self-adjoint.

Variation of h gives the following condition of stationarity of the functional π^* in eqn (12) if we use the result (A16) and introduce the moment tensor $M^{\alpha\beta}(h, w)$ given by eqn (2),

$$\int_\Omega w d_\alpha d_\beta \delta M^{\alpha\beta}(h, w)\, d\Omega + \int_\Omega [-\Lambda + \lambda - \kappa]\delta h\, d\Omega = 0. \tag{A17}$$

Treating the first term in analogy with our manipulation of the second term in eqn (A1) during the steps from eqn (A1)–(A6), we obtain

$$-\oint_\omega w\delta Q(h, w)\, d\omega + \sum_I \{w\delta Q^*(h, w)\}_{x^* = x_I^*} - \oint_\omega \Psi(w)\delta M_B(h, w)\, d\omega$$

$$+ \int_\Omega \delta M^{\alpha\beta}(h, w) d_\alpha d_\beta w\, d\Omega + \int_\Omega [-\Lambda + \lambda - \kappa]\delta h\, d\Omega = 0, \tag{A18}$$

but here, the three first terms vanish for any of the sets of boundary conditions (5a), (5b) or (5c) under consideration. Now, writing $\delta M^{\alpha\beta}$ as $\delta(DM^{\alpha\beta}/D)$, noting that $M^{\alpha\beta}/D$ does not contain h, and using the well known result[28] that the tensor $d_\alpha d_\beta w$, i.e. the covariant curvature tensor, can be expressed in terms of the moment tensor as

$$d_\alpha d_\beta w = \frac{1}{(1-\nu^2)D} [(1+\nu)M_{\alpha\beta} - \nu a_{\alpha\beta}M_\gamma{}^\gamma], \tag{A19}$$

we obtain the following equation by performing the variation with respect to h in eqn (A18) and collecting terms,

$$\int_\Omega \left\{\frac{dD}{dh}\frac{1}{(1-\nu^2)D^2}[(1+\nu)M^{\alpha\beta}M_{\alpha\beta} - \nu M_\alpha{}^\alpha M_\beta{}^\beta] - \Lambda + \lambda - \kappa\right\}\delta h\, d\Omega = 0. \tag{A20}$$

Since δh is arbitrary, we thus have

$$\frac{dD}{dh}\frac{1}{(1-\nu^2)D^2}[(1+\nu)M^{\alpha\beta}M_{\alpha\beta} - \nu M_\alpha{}^\alpha M_\beta{}^\beta] = \Lambda - \lambda + \kappa, \tag{A21}$$

which constitutes the optimality condition for our problem.